Published in final edited form as:
Mol Genet Metab. 2010 ; 101(2-3): 183–191. doi:10.1016/j.ymgme.2010.07.008.

An animal model of PDH deficiency using AAV8-siRNA vector-mediated knockdown of pyruvate dehydrogenase E1α

Carolyn Ojano-Dirain[1], **Lyudmyla G. Glushakova**[1], **Li Zhong**[2,4], **Sergei Zolotukhin**[2,3,4], **Nicholas Muzyczka**[2,3], **Arun Srivastava**[2,3,4], and **Peter W. Stacpoole**[1,5,*]

[1] Division of Endocrinology and Metabolism, Department of Medicine, University of Florida, Gainesville, FL, 32610, USA

[2] Powell Gene Therapy Center and Genetics Institute, University of Florida, Gainesville, FL, 32610, USA

[3] Department of Molecular Genetics and Microbiology, University of Florida, Gainesville, FL, 32610, USA

[4] Division of Cellular and Molecular Therapy, Department of Pediatrics, University of Florida, Gainesville, FL, 32610, USA

[5] Department of Biochemistry and Molecular Biology, University of Florida, Gainesville, FL, 32610, USA

Abstract

We evaluated the feasibility of self-complementary adeno-associated virus (scAAV) vector-mediated knockdown of the pyruvate dehydrogenase complex using small interfering RNAs directed against the E1α subunit gene (PDHA1). AAV serotype 8 was used to stereotaxically deliver scAAV8-si3-PDHA1-Enhanced Green Fluorescent Protein (knockdown) or scAAV8-EGFP (control) vectors into the right striatum and substantia nigra of rats. Rotational asymmetry was employed to quantify abnormal rotation following neurodegeneration in the nigrostriatal system. By 20 weeks after surgery, the siRNA-injected rats exhibited higher contralateral rotation during the first 10 min following amphetamine administration and lower 90-min total rotations ($p \leq 0.05$). Expression of PDC E1α, E1β and E2 subunits in striatum was decreased ($p \leq 0.05$) in the siRNA-injected striatum after 14 weeks. By week 25, both PDC activity and expression of E1α were lower ($p \leq 0.05$) in siRNA-injected striata compared to controls. E1α expression was associated with PDC activity ($R^2=0.48$; $p=0.006$) and modestly associated with counterclockwise rotation ($R^2=0.51$;$p=0.07$). The use of tyrosine-mutant scAAV8 vectors resulted in ~17-fold increase in transduction efficiency of rat striatal neurons *in vivo*. We conclude that scAAV8-siRNA vector-mediated knockdown of PDC E1α in brain regions typically affected in humans with PDC deficiency results in a reproducible biochemical and clinical phenotype in rats that may be further enhanced with the use of tyrosine-mutant vectors.

[*]To whom correspondence should be addressed at P.O. Box 100226, University of Florida College of Medicine, Gainesville, FL 32610, USA. Tel: 352-273-9023, Fax: 352-273-9013, pws@ufl.edu.

Keywords

PDC, pyruvate dehydrogenase complex; scAAV, self-complementary adeno-associated virus; EGFP, enhanced green fluorescent protein; siRNA, small interfering ribonucleic acid; animal model; rare disease

1.1. INTRODUCTION

The pyruvate dehydrogenase complex (PDC) is a mitochondrial enzyme that plays a central role in aerobic energy metabolism by catalyzing the irreversible oxidation of glucose-derived pyruvate to acetyl-CoA. The complex is entirely nuclear encoded and comprises multiple copies of three structurally distinct, but functionally interdependent, enzymes (E_1 through E_3) [1]. Pyruvate dehydrogenase (E1; EC 1.2.4.1) is a heterotetrameric ($\alpha_2\beta_2$) α-keto acid decarboxylase that oxidizes pyruvate to acetyl CoA and requires thiamine pyrophosphate as cofactor; dihydrolipoamide acetyltransferase (E2; EC 2.3.1.12) forms the structural core of the complex; and dihydrolipoamide dehydrogenase (E3; EC 1.8.1.4) is a flavoprotein enzyme that is stably integrated into the complex by an E3-binding protein (E3bp). Rapid regulation of PDC activity occurs by product inhibition and by reversible phosphorylation of serine residues on the E1α subunit that is mediated by a family of PDC kinases (PDK) and phosphatases (PDP) [2,3].

Inborn errors of the PDC are among the more common causes of congenital lactic acidoses [4,5]. Because the PDC catalyzes the first step in the mitochondrial metabolism of carbohydrate, inhibition of pyruvate decarboxylation severely impairs the yield of ATP from glucose and leads to accumulation of lactate and pyruvate. Highly oxidative tissues, such as the central nervous system (CNS), are particularly vulnerable to loss of PDC activity. Thus, the most prevalent clinical manifestations of PDC deficiency reflect progressive neuromuscular and neurobehavioral deterioration, such as mental retardation and developmental delay, hypotonia, exercise intolerance, motor disorders and seizures [5,6]. Indeed, the biochemical and clinical manifestations of PDC deficiency may appear to reflect solely CNS involvement without significant extracranial complications [7]. PDC deficiency is also one of several inborn errors of mitochondrial energetics that may lead to the characteristic neuropathology of Leigh syndrome, with spongy degeneration in the thalamus, basal ganglia and brain stem [7,8]. By far the majority of biochemically proven cases of PDC deficiency are due to defects in the X-linked E1α subunit gene (*PDHA1*) [9].

There are no proven treatments for PDC deficiency. The recent development of a murine model of the disease demonstrates that complete deficiency of PDC E1α is a lethal defect for the developing male embryo [10,11]. Conditional knockout strategies offer a potential alternative to the more traditional embryonic cell knockout approach. Ribozymes can be used for direct delivery of genes using viral vectors, such as the nonpathogenic human adeno-associated virus 2 (AAV2), and to down-regulate genes *in vivo* in creating animal models of disease [12]. Although hammerhead ribozymes can cause knockdown of E1α activity *in vitro* [13], such an action could not be replicated *in vivo* (unpublished observations). Therefore, we adopted an alternative approach to knockdown the pyruvate dehydrogenase E1α gene (*PDHA1*) by using a combination of self-complementary AAV (scAAV) vector and RNA interference technologies. Delivery of small interfering RNA (siRNA) using scAAV vectors can produce sustained knockdown of *PDHA1* gene in transduced cells *in vitro* [14]. Moreover, scAAV vectors can be used to deliver and express *PDHA1* in cultured mammalian cells and partially restore PDC activity in defective cells [15].

Here we determined the feasibility of recombinant scAAV8-mediated knockdown of PDC E1α using siRNAs directed against the *PDHA1* in the striatum (ST) and substantia nigra (SN) of rats. We also developed capsid-modified tyrosine-mutants that are capable of high-efficiency transduction in the rat striatum *in vivo*.

2.1. MATERIALS AND METHODS

2.1.1. Construction of the recombinant AAV vector encoding siRNA and virus preparation

The design and construction of scAAV-based plasmid encoding siRNA to target rat PDHA1 sequences was described previously [14]. The plasmid construct includes the EGFP gene driven by a chicken β-actin (CBA) promoter [16]. Vectors were packaged at the University of Florida Powell Gene Therapy Center. Vector titer (viral particles/mL) were determined by dot-blot hybridization analysis. The titers of scAAV8-EGFP and scAAV8-si3-PDHA1-EGFP were 3.3×10^{11} and 4.89×10^{12} viral genomes/mL, respectively.

2.1.2. Construction of surface-exposed tyrosine residue mutant AAV8 capsid plasmid

We utilized a procedure based on the QuikChangeII site-directed mutagenesis (Stratagene, La Jolla, CA) according to the manufacturer's protocol and as we previously described [17]. The nucleotide sequences of primers used for site-directed mutagenesis of surface-exposed tyrosine residues are shown in Table 1. The introduction of tyrosine to phenylalanine (Y-F) mutations was confirmed by DNA sequencing. The titers of scAAV8-Y447F-EGFP and scAAV8-Y733F-EGFP were 1.6×10^{12} and 2.7×10^{12} viral genomes/mL, respectively.

2.1.3. Animal surgeries

All surgical procedures and care were approved by the UF Institutional Animal Care and Use Committee. The brain coordinates (calculated relative to the bregma) for injections for the ST were: anterior-posterior (AP) −0.5 mm, medial-lateral (ML) −3.5 mm, and dorso-ventral (DV) −5.0 mm from dura. For the SN, the coordinates were: AP +5.6 mm, ML −2.4 mm, and DV −7.2 mm from dura. Briefly, after the rats were anesthetized, they were placed in a stereotaxic frame (Kopf Instruments, Tujunga, CA) and received a subcutaneous injection of marcaine at the incision site. Rats were continuously under isoflurane anesthesia during the injection procedure. Injections were performed with a 5-μl Hamilton syringe fitted with a glass micropipette with an opening of approximately 60–80 μm. Vectors were injected at a rate of 0.5 μl/min. The titer of vector stocks were adjusted to attain the same titer for each vector. For SN injections, the needle was left in place for 5 min before being slowly removed from the brain. For ST injections, the needle was retracted an additional 1 mm 1 min after the cessation of the injection and was then left in place for an additional 4 min before being slowly withdrawing it from the brain.

2.1.4. Recombinant AAV-mediated siRNA vector-mediated knockdown of PDC E1α in the striatal and nigral regions of the rat brain

Fifteen female Sprague-Dawley rats (225–250g, Charles River Laboratories) underwent stereotaxic surgery (described above) into the right striatum (1.5×10^{10} viral particles) and substantia nigra (7.3×10^{9} viral particles) to deliver scAAV8-si3-PDHA1-EGFP (n=10, PDHA1 knockdown) or scAAV8-EGFP (n=5, positive control) vectors. Five rats served as negative controls (no surgery). The left (uninjected) hemisphere was used as control tissue from each rat for the biochemical and immunohistochemical assays. Animals were monitored weekly and showed no difference in body weight over a 6-month period of observation.

2.1.5. Rotational behavior

Rotational activity was monitored starting 4 weeks after surgery by intraperitoneally injecting animals with 2.5 mg/kg amphetamine sulfate (Sigma-Aldrich, St. Loius, MO). Amphetamine causes neuronal release of dopamine that leads to measurable changes in rotational behavior in rats. This technique has become a standard and robust method for quantifying abnormal behavior following chemical or genetically-induced neurodegeneration in the rat nigrostriatal system [18–21]. Animals were fitted with small, non-restricting harnesses and placed in automated rotometer bowls [22]. Full 360 clockwise and counterclockwise rotations were measured during a 90-min period after amphetamine injection.

2.1.6. Tissue processing for biochemical and immunohistochemical studies

After 14 weeks, 5 PDHA1-siRNA-injected rats and 3 rats from each control group were sacrificed for tissue analyses. The remaining rats, 5 siRNA-injected and 2 rats from each control, were followed until week 24 and were sacrificed for tissue analyses on week 25.

Rats were deeply anesthetized with pentobarbital and decapitated. The brains were rapidly removed and sectioned coronally at the level of the cerebral peduncles. The ST were dissected from the region anterior to the cut while the SN were dissected from the region posterior to the cut. The left and right ST were separated and isolated from the surrounding tissue. The tissue from each ST hemisphere was homogenized and separated into two tubes, sample weights were recorded and specimens were quickly frozen in liquid nitrogen. Tissues were stored in −80°C until further biochemical analyses. On the other hand, the brain section containing the SN were post-fixed for 24 h in 4% paraformaldehyde in 0.01 M PBS and then transferred to a 30% sucrose in 0.01 M PBS solution. Brains are cut into 40 μm thick coronal sections using a freezing stage sliding microtome. SN tissue sections were used for immunohistochemical staining.

2.1.7. PDC activity

Striatal tissues were analyzed for PDC activity by measuring the rate of $^{14}CO_2$ formation from [1-^{14}C]-labeled pyruvate [14,23]. Six hundred microliter of KCl-MOPS buffer (80 mM KCl, 50 mM MOPS, 2 mM $MgCl_2$, 0.5 mM EDTA, pH 7.4) with serine protease inhibitors (Leupeptin and PMSF) were added per 30 mg of pre-weighed tissue. Tissue was homogenized thoroughly by hand for at least 30 seconds in a 1 ml Kontes Duall glass tissue grinder and centrifuged at 1,000*x*g for 10 min at 4°C. Tissue homogenates were subjected to repeated freezing and thawing to complete tissue disruption. Homogenates (100 μL/sample) were then incubated for 15 min at 37°C with 7.5 μL PDH phosphatase (Sigma, St. Louis, MO) and 10 μL of DCA (125 mM):$MgCl_2$ (0.5 M):$CaCl_2$ (50 mM) mixed at 2:1:1 ratio. Reactions were halted by addition of a stop solution (25mM NaF, 25mM EDTA, 4mM dithiothreitol, 40% ethanol). Each sample was run in quadruplicate, with appropriate blanks. Protein concentrations were determined by a Bradford protein assay and the specific activity of ^{14}C-pyruvate was expressed as nmol $^{14}CO_2$ produced/min/mg protein.

2.1.8. Western blotting

Protein expression of the PDC subunits (E1α, E1β, E2, E2/E3 binding protein) was measured by Western immunoblotting using primary monoclonal antibodies (MitoSciences, Inc., Eugene, OR). Our previous studies in fibroblasts from PDC E1α-deficient patients indicated that reactive oxygen species accumulate in these cells [24]. Therefore, protein expression of the mitochondrial oxygen free radical scavenger MnSOD was measured as an index of oxidant stress. We also determined the protein expression of tyrosine hydroxylase (TH), a marker of dopaminergic neurons.

Protein concentrations were determined by a Bradford assay and samples were normalized according to protein concentration. Protein lysates were separated on 10, 15 or 4–20% SDS–polyacrylamide gels (Lonza, Rockland, ME) and transferred to PVDF membranes (GE Healthcare Biosciences Corp., Piscataway, NJ). After transfer, the membranes were blocked with 5% non-fat milk (Bio-Rad Laboratories, Hercules, CA) in PBS overnight at 4°C with gentle agitation and then probed for 2h at room temperature or overnight at 4°C with primary antibodies diluted in 1% milk/PBS. After four 5-min washes in PBS/0.05% Tween-20, the membranes were incubated with appropriate secondary antibodies (horseradish peroxidase-conjugated goat anti-mouse IgG or goat anti-rabbit IgG, Santa Cruz Biotechnology, Inc., Santa Cruz, CA) for 1h at room temperature. After four 5-min washes in PBS/0.05%Tween-20, proteins are detected using chemiluminescent substrate (SuperSignal West Pico Chemiluminescent Substrate, Thermo Scientific, Rockford, IL) according to the manufacturer's instructions. The amount of protein was standardized to the amount of α-tubulin in each lane.

2.1.9. Immunohistochemistry and stereological cell counts

Floating SN sections (40μm) were washed with 0.01 M PBS and then treated for 15 min with 0.5% H_2O_2+10% methanol in 0.01 M PBS. The sections were preincubated with 3% normal horse serum (NHS)+0.1% Triton X-100 in 0.01 M PBS and then incubated overnight at room temperature with a 1:2,000 dilution of a mouse anti-TH antibody (Chemicon, Temecula, CA). Sections were washed and incubated for 2h at room temperature with a biotinylated anti-mouse secondary antibody. The reactions were visualized using an avidin–biotin peroxidase complex (Vector Laboratories, Burlingame, CA) followed by incubation with NovaRED substrate (Vector Laboratories, Burlingame, CA). Sections were mounted on subbed slides, dehydrated in ascending alcohol concentrations, cleared in xylene and coverslipped.

Unbiased stereological cell counts of the total number of TH positive neurons in the SN were performed using the optical fractionator method as previously described [25]. This sampling technique is not affected by tissue volume changes and does not require reference volume determinations. Sampling of cells was performed using the MicroBrightfield StereoInvestigator System (Williston, VT). The software was used to outline the SN or ST area using a 5x objective and generate counting areas by placing counting grids (100 μm×100 μm) in the outlined area. A counting frame was randomly and systematically moved through the counting area until the entire delineated area was sampled. Actual counting was performed using the 100x objective. The total number of TH positive cells was estimated using the optical fractionator formula [25] and the coefficient of error was calculated according to Gundersen and Jenson [26]. The person performing the counts was blinded as to the identity of the treatment group.

2.1.10. Transduction efficiency of novel tyrosine-mutant AAV8 vectors

We tested the transduction efficiency of two AAV8 tyrosine mutants, Y447F and Y733F, in which the surface tyrosine residues 447 and 733 that correspond to residues 444 and 730 in AAV2 were mutated [17]. We injected the left striatum of rats with 2×10^{10} vector genome of Y447F-scAAV8-EGFP or Y733F-scAAV8-EGFP while the right striatum was injected with wild-type scAAV8-EGFP (n=3 per group). After 6 weeks, rats were sacrificed. The striatum was excised, sectioned and checked for GFP fluorescence using fluorescent microscopy. Images from 3 to 4 visual fields per animal were analyzed quantitatively by ImageJ analysis software. Transgene expression was analyzed and compared with the wild-type scAAV8-EGFP within the same treatment.

2.1.11. Statistical analyses

Differences between groups were compared using the group-paired Student's t-test or analysis of variance (ANOVA) (JMP 7.0, SAS Institute Inc., Cary, NC). Correlations were made using regression analyses. Data are presented as the mean ± SEM and $p \leq 0.05$ was considered statistically significant.

3.1. RESULTS

3.1.1. Transgene expression of wild-type scAAV8 vector

Transgene expression in the SN was visualized with fluorescent microscopy, while GFP transgene expression in the ST was detected with immunoblotting. As shown in Fig. 1, transgene expression persisted for the duration of the experiments (25 weeks). There were no GFP fluorescent cells in the uninjected SN (not shown) or GFP protein in the left (uninjected) ST (Fig. 1B). GFP was more highly localized in the SN than in the ST, possibly reflecting the different anatomical volumes of these regions. Localization was similar to that achieved in other rodent models of neurodegenerative diseases [27–29].

3.1.2. Amphetamine-induced rotational behavior

Rotational behavior has been successfully utilized by us and our colleagues to characterize animal models involving neurodegeneration (loss of dopaminergic neurons) in the nigrostriatal system [18–20]. There was no difference in rotational behavior among the three animal groups up to week 16. However, the contralateral rotation of *PDHA1* knockdown rats increased during the first 10 min following amphetamine administration, compared to that observed in either control group 20 and 24 weeks after vector injection into the nigrostriatal area of the right hemisphere ($p \leq 0.05$; Fig. 2A). Rats that received the *PDHA1*-siRNA also showed markedly less motor activity than controls 20 to 90 min after amphetamine injection (Fig. 2B).

3.1.3. PDH activity and protein expression

Striatal tissue was analyzed for PDC activity by measuring the oxidation of $^{14}CO_2$ from [1-^{14}C] pyruvate [14,23] and for expression of various proteins by Western immunoblotting. At 14 weeks, there was no difference in PDC activity between the ipsilateral (injected) and contralateral striata in rats receiving AAV8-EGFP but there was a trend (p=0.09) toward lower PDC activity in the ipsilateral side of striata from siRNA-injected rats (Fig. 3A). PDC E1α expression was decreased 20% (p=0.02) in the right striatum of siRNA-injected rats, compared to the left ST of these animals or to the right ST of GFP-injected controls (Fig. 3B). The expression of PDC E1β and E2, but not of the PDC E2/E3 binding protein, were also decreased (p<0.05) in the right ST of siRNA-injected rats, compared to left ST or to the right ST of controls (Figs. 3C and 3D). In addition, expression of the mitochondrial antioxidant manganese superoxide dismutase (MnSOD) was also lower ($p \leq 0.001$) in the siRNA-injected striata (Fig. 3E)

By week 25, both the activity and expression of PDC E1α were lower (both $p \leq 0.05$) in siRNA-injected striata than in the contralateral or GFP-injected tissue (Figs. 4A and 4B). PDC activity was associated with E1α expression (R^2=0.48; p=0.006) when the data from the siRNA and GFP-injected tissues were combined. There was a more modest association between E1α expression and contralateral rotation (R^2=0.51; p=0.07).

3.1.4. Nigrostriatal TH positive (dopaminergic) neurons

The number of TH expressing neurons in the SN was evaluated as a marker for DA neurons. A representative section of SN from scAAV8-EGFP (left panel) and scAAV8-si3PDHA1-EGFP (right panel) injected rats showing staining of TH positive (+) neurons is shown in Fig.

5A. The number of TH+ neurons, measured by unbiased stereological cell count, was 35% lower ($p \leq 0.005$) in the PDHA1 siRNA injected SN compared to the uninjected SN of these rats (Fig. 5B).

3.1.5. Tyrosine-mutant AAV8 vector-mediated transduction

While the current experiments were on-going, we demonstrated that site-directed mutagenesis of surface-exposed tyrosine residues on AAV2 capsids resulted in significantly higher transduction efficiency of mammalian cells *in vivo* and *in vitro* compared with the wild-type (WT) vector [17,30]. To evaluate whether this approach can be adapted to achieve better transduction of rat striatum CNS cells, we tested the transduction efficiency of two AAV8 tyrosine mutants, Y447F and Y733F, in which the surface tyrosine residues 447 and 733 that correspond to residues 444 and 730 in AAV2 were mutated [17]. We injected the left ST of rats with 2×10^{10} vector genome of Y447F-scAAV8 or Y733F-scAAV8 while the right ST was injected with wild-type scAAV8-EGFP (n=3 per group). After 6 weeks, rats were sacrificed. The ST was excised, sectioned and checked for GFP fluorescence using fluorescent microscopy (Fig. 6, Panel A). Images from 3 to 4 visual fields per animal were analyzed quantitatively by ImageJ analysis software. Transgene expression was analyzed and compared with the WT scAAV8-EGFP within the same treatment. The transgene expression of the WT scAAV8-EGFP vector was similar in both treatment groups (Fig. 6, Panel B). The transduction efficiency of Y447F and Y733F vectors was 4- and 17-fold higher than the WT vector, respectively (Fig. 6, Panel B).

4.1. DISCUSSION AND CONCLUSION

Neurodegeneration in the basal ganglia, which comprise the ST (putamen and caudate nucleus), globus pallidus, subthalamic nucleus and SN, is a hallmark of PDC deficiency [7,8]. Recombinant AAV8 efficiently transduces neurons in the basal ganglia [31,32] and small interfering RNAs (siRNAs) have also been widely employed to induce knockdown of reactive genes when delivered to discrete tissues *in vivo*. The selectivity of AAV8 for neuronal cells is not a drawback because neurons are likely the most vulnerable CNS cell type to interruption of mitochondrial oxidative metabolism. Indeed, brain neurons typically utilize both glucose and lactate, the latter derived from astroglial glycolysis, to sustain function [33]. Both energy substrates yield pyruvate and, hence, require a functional PDC to contribute to neuronal oxidative phosphorylation. Therefore, it is reasonable to postulate that siRNAs designed to interact specifically with the E1α messenger RNA (mRNA) and delivered via local injection of rAAV8 to these brain regions might recapitulate the neuropathology of PDC deficiency. One clear advantage of this potential animal model is that it lacks the embryonic lethality in male rodents that results from germline knockout of PDC [10]. Furthermore, if this system functions appropriately in rodents, it can rapidly be adapted to larger species, such as primates, with more potential applicability to the human syndrome.

Accordingly, we first designed siRNAs to cleave the mRNA of the E1α subunit and tested them *in vitro* to assess the feasibility of producing a gene knockdown in rats [14]. In this study we used AAV8 vector-mediated delivery of a PDC E1α siRNA to knockdown PDC E1α in rat ST and SN. Similar to the *in vitro* studies, we employed double-stranded DNA that contained self-complementary AAV vectors to eliminate the requirement of viral second-strand DNA synthesis and thus increase the efficiency of transgene expression [14].

A significant decrease in E1α protein expression in the *PDHA1* knockdown animals was observed 14 weeks after delivery of the viral vector whereas significant knockdown of PDC activity occurred after 24 weeks. The reduction in E1α protein expression was accompanied with a reduction in the E1β and E2 expression. This would be expected because the E1α protein

is regarded as necessary for normal assembly of the heterotetrameric E1($\alpha_2\beta_2$) component itself and subsequent formation of the multimeric enzyme complex [34,35].

We previously reported that production of reactive oxygen species is increased and that expression of the mitochondrial antioxidant MnSOD is decreased in primary cultures of fibroblasts from PDC-deficient patients [24]. A lower expression of MnSOD was observed in the injected hemisphere of PDHA1 knockdown rats compared to both the uninjected hemisphere and to the injected side of the controls, consistent with our findings in fibroblasts from affected patients. A profound MnSOD protein loss was also observed in cerebral endothelial cells exposed to moderate oxidative stress for 24 h [36]. Thus, the lower expression of MnSOD in fibroblasts from PDC-deficient patients and in the *PDHA1* knockdown rats may reflect oxidant stress induced by the PDC-deficient state and lead to further inactivation of PDC by reactive oxygen species [37].

Successful knockdown of PDC E1α should lead to neurodegeneration and therefore to loss of neurons. Using amphetamine-induced rotation, a standard method for quantifying abnormal rotational behavior following neurodegeneration of the nigrostriatal system [18–20], we observed a higher contralateral rotation in the *PDHA1*-siRNA injected rats during the first 10-min after amphetamine injection compared to the control animals, although this difference was not maintained during the remaining period of observation. However, siRNA-injected rats showed a substantial decrease in overall movement, suggesting a sustained effect on animal behavior from *PDHA1* knockdown. Moreover, only the *PDHA1*-siRNA-injected rats exhibited a significant rotational bias. This observation concurs with previous reports indicating that control or non-lesioned rats are expected to have no net rotations in one direction [18]. We also observed that 20 to 90 min after the amphetamine injection, the PDHA1 knockdown rats showed decreased total rotational behavior. The asymmetric behavior of the *PDHA1* knockdown rats could be attributed to the decreased number of surviving dopaminergic neurons in the injected SN. Unbiased stereological cell count of nigral sections showed a significant decrease in TH-positive cells in the SN injected with AAV8-si3PDHA1-EGFP.

This is the first report to indicate that a rotational test of movement previously demonstrated in other animal models can be used to correlate aberrant behavior with targeted disruption of PDC in the CNS. It has been estimated that the activity of PDC in mammalian brain is near-maximal (i.e., the E1α subunit is almost completely unphosphorylated) to meet the high energy demands of neuronal cells; therefore, even modest inhibition of enzyme activity would lead to functional CNS pathology [7]. This notion is consistent with our observation that ~20% reduction in PDC activity (Fig. 4A) is sufficient to induce significant behavioral changes and with previous findings in which a 24% decrease in PDH activity in the dorsolateral striatum of rats subjected to forebrain ischemia led to extensive delayed neuronal loss [38]. Thus, the present study serves as proof of principal of the utility of AAV8-siRNA vector-mediated knockdown of PDHA1 in developing an animal model of PDC deficiency. Future experiments are warranted to determine the extent of *PDHA1* knockdown from delivery of larger vector titers or from multiple injections of vector in select brain regions.

While the current study was on-going, our group demonstrated that mutations of tyrosine residues of AAV2 capsids lead to increased ubiquitination transduction efficiency [16]. When we tested the transduction efficiency of two AAV8 tyrosine mutants, Y447F and Y733F, in which the surface tyrosine residues 447 and 733 that correspond to residues 444 and 730 in AAV2 were mutated [cf. 17], Y733F also dramatically improved transduction efficiency of striatal neurons compared to WT scAAV8 vector. The transduction efficiency of Y447F and Y733F vectors was markedly higher than efficiency obtained with the WT vector. We hypothesize that these tyrosine-mutant vectors can be used to optimize the scAAV8-siRNA vector-mediated knockdown of PDC activity and E1α expression to develop a more robust

animal model of PDC deficiency. Moreover, AAV serotypes show selective tissue and cell tropism [39–41]. Thus, various combinations of tyrosine-mutant AAV vectors may be employed in future experiments to generate both global and tissue- or organ-specific PDC deficiency as well as targeted high-efficiency delivery of therapeutic genes.

Acknowledgments

This work was supported in part by NIH grant 1UL1RR029890-01 (Clinical and Translational Science Award). We thank Kathryn St. Croix and Candace Caputo for editorial assistance.

References

1. Smolle M, Prior AE, Brown AE, Cooper A, Byron O, Lindsay JG. A new level of architectural complexity in the human dehydrogenase complex. J Biol Chem 2006;281:19772–19780. [PubMed: 16679318]
2. Holness MJ, Sugden MC. Regulation of pyruvate dehydrogenase complex activity by reversible phosphorylation. Biochem Soc Trans 2003;31:1143–1151. [PubMed: 14641014]
3. Reed LJ. Regulation of mammalian pyruvate dehydrogenase complex by a phosphorylation-dephosphorylation cycle. Curr Top Cell Regul 1981;18:95–106. [PubMed: 7273851]
4. Stacpoole PW, Barnes CL, Hurbanis MD, Cannon SL, Kerr DS. Treatment of congenital lactic acidosis with dichloroacetate. Arch Dis Child 1997;77:535–541. [PubMed: 9496194]
5. Stacpoole, PW. The congenital lactic acidoses. In: Winters, R., editor. NORD Guide to Rare Disorders. Lippincott, Williams & Wilkins; Philadelphia, PA: 2003. p. 462-464.
6. Brown GK, Brown RM, Scholem RD, Kirby DM, Dahl HHM. The clinical and biochemical spectrum of human pyruvate dehydrogenase complex deficiency. Ann NY Acad Sci 1989;573:360–368. [PubMed: 2517465]
7. Robinson, BH. Lactic acidemia: disorders of pyruvate carboxylase and pyruvate dehydrogenase. In: Scriver, CR.; Beaudet, AL.; Sly, WS.; Valle, D., et al., editors. The Metabolic & Molecular Bases of Inherited Disease. Vol. II. McGraw-Hill; New York: 2001. p. 2275-2295.
8. Leigh D. Subacute necrotizing encephalomyopathy in an infant. J Neurol Neurosurg Psychiatry 1951;14:216–221. [PubMed: 14874135]
9. Lissens W, De Meirleir L, Seneca S, Liebaers I, Brown GK, Brown RM, et al. Mutations in the X-linked pyruvate dehydrogenase (E1) subunit gene (*PDHA1*) in patients with a pyruvate dehydrogenase complex deficiency. Hum Mutat 2000;15:209–219. [PubMed: 10679936]
10. Johnson MT, Mahmood S, Hyatt SL, Yang HS, Soloway PD, Hanson RW, et al. Inactivation of the murine pyruvate dehydrogenase (PDCa1) gene and its effect on early embryonic development. Mol Genet Metab 2001;74:293–302. [PubMed: 11708858]
11. Sukhdeep S, Gangasani A, Korotchkina LG, Suzuki G, Fallavollita JA, Canty JM Jr, et al. Tissue-specific pyruvate dehydrogenase complex deficiency causes cardiac hypertrophy and sudden death of weaned male mice. Am J Physiol Heart Circ Physiol 2008;295:946–952.
12. Lewin AS, Hauswirth WW. Ribozyme gene therapy: applications for molecular medicine. Trends Mol Med 2001;7:221–228. [PubMed: 11325634]
13. Han, Z.; Harrison, JC.; Thomas, J., Jr, et al. Preliminary study of hammerhead ribozyme-mediated knockdown of rat PDC E1α mRNA. SIMD Annual Meeting; Orlando, FL. March 7–10, 2004;
14. Han Z, Gorbatyuk M, Thomas J Jr, Lewin AS, Srivastava A, Stacpoole PW. Down-regulation of rat pyruvate dehydrogensae E1α gene by self-complementary adeno-associated virus-mediated small interfering RNA delivery. Mitochondrion 2007;7:253–259. [PubMed: 17392036]
15. Han Z, Berendzen K, Zhong L, Surolia I, Chouthai N, Zhao W, et al. A combined therapeutic approach for pyruvate dehydrogenase deficiency using self-complementary adeno-associated virus serotype-specific vectors and dichloroacetate. Mol Genet Metab 2008;93:381–387. [PubMed: 18206410]
16. Zhong L, Zhao W, Wu J, Li B, Zolotukhin S, Govindasamy L, et al. A Dual role of EGFR protein tyrosine kinase signaling in ubiquitination of AAV2 capsids and viral second-strand DNA synthesis. Mol Ther 2007;15:1323–1330. [PubMed: 17440440]

17. Zhong L, Li B, Mah CS, Govindasamy L, Agbandje-McKenna M, Cooper M, et al. Next generation of adeno-associated virus 2 vectors: point mutations in tyrosines lead to high-efficiency transduction at lower doses. Proc Nat Acad Sci USA 2008;105:7827–7832. [PubMed: 18511559]

18. Kirik D, Rosenblad C, Bjorklund A, Mandel RJ. Long-term rAAVmediated gene transfer of GDNF in the rat Parkinson's model: intrastriatal but not intranigral transduction promotes functional regeneration in the lesioned nigrostriatal system. J Neurosci 2000;20:4686–4700. [PubMed: 10844038]

19. Kirik D, Georgievska B, Burger C, Winkler C, Muzyczka N, Mandel RJ, et al. Reversal of motor impairments in parkinsonian rats by continuous intrastriatal delivery of L-dopa using rAAV-mediated gene transfer. Proc Natl Acad Sci USA 2002;99:4708–4713. [PubMed: 11917105]

20. Manfredsson F, Burger C, Sullivan L, Muzyczka N, Lewin AS, Mandel RJ. rAAV-mediated nigral human parkin over-expression partially ameliorates motor deficits via enhanced dopamine neurotransmission in a rat model of Parkinson's disease. Exp Neurol 2007;207:289–301. [PubMed: 17678648]

21. Schallert S. Behavioral tests for preclinical intervention assessment. J Am Soc Exp Neurotherapeutics 2206;3:497–504.

22. Ungerstedt U, Arbuthnott GW. Quantitative recording of rotational behavior in rats after 6-hydroxy-dopamine lesions of the nigrostriatal dopamine system. Brain Res 1970;24:485–493. [PubMed: 5494536]

23. Simpson NE, Han Z, Berendzen KM, Sweeney CA, Oca-Cossio JA, Constantinidis I, et al. Magnetic resonance spectroscopic investigation of mitochondrial fuel metabolism and energetics in cultured human fibroblasts: effects of pyruvate dehydrogenase complex deficiency and dichloroacetate. Mol Genet Metab 2006;89:97–105. [PubMed: 16765624]

24. Judge, S.; Pourang, D.; Stacpoole, PW. Apoptotic cell death is increased in fibroblasts from pyruvate dehydrogenase deficient individuals. UMDF Annual Meeting; Indianapolis, IN. June 25–28, 2008;

25. West MJ, Slomianka L, Gundersen HJ. Unbiased stereological estimation of the total number of neurons in the subdivisions of the rat hippocampus using the optical fractionators. Anat Rec 1991;231:482–497. [PubMed: 1793176]

26. Gundersen HJ, Bagger P, Bendtsen TF, Evans SM, Korbo L, Marcussen N, et al. The new stereological tools: dissector, fractionator, nucleator and point sampled intercepts and their use in pathological research and diagnosis. APMIS 1988;96:857–881. [PubMed: 3056461]

27. Kirik D, Georgievska B, Burger C, Winkler C, Muzyczka N, Mandel RJ, et al. Reversal of motor impairments in parkinsonian rats by continuous intrastriatal delivery of L-dopa using rAAV-mediated gene transfer. Proc Natl Acad Sci USA 2002;99:4708–4713. [PubMed: 11917105]

28. Manfredsson F, Burger C, Sullivan L, Muzyczka N, Lewin AS, Mandel RJ. rAAV-mediated nigral human parkin over-expression partially ameliorates motor deficits via enhanced dopamine neurotransmission in a rat model of Parkinson's disease. Exp Neurol 2007;207:289–301. [PubMed: 17678648]

29. Reimsnider S, Manfredsson F, Muzyczka N, Mandel RJ. Time course of transgene expression after intrastriatal pseudotyped rAAV2/1, rAAV2/2, rAAV2/5 and rAAV2/8 transduction in the rat. Mol Ther 2007;15:1504–1511. [PubMed: 17565350]

30. Petrs-Silva H, Dinculescu A, Li Q, Min SH, Chiodo V, Pang J, et al. High-efficiency transduction of the mouse retina by tyrosine-mutant AAV serotype vectors. Mol Ther 2009;17:463–471. [PubMed: 19066593]

31. Reimsnider S, Manfredsson F, Muzyczka N, Mandel RJ. Time course of transgene expression after intrastriatal pseudotyped rAAV2/1, rAAV2/2, rAAV2/5 and rAAV2/8 transduction in the rat. Mol Ther 2007;15:1504–1511. [PubMed: 17565350]

32. McFarland NR, Lee JS, Hyman BT, McLean P. Comparison of transduction efficiency of recombinant AAV serotypes 1, 2, 5 and 8 in the rat nigrostriatal system. J Neurochem 2009;109:838–845. [PubMed: 19250335]

33. Rouach N, Koulakoff A, Abudara V, Willecke K, Giaume C. Astroglial metabolic networks sustain hippocampal synaptic transmission. Science 2008;322:1551–1555. [PubMed: 19056987]

34. Seyda A, McEachern G, Haas R, Robinson BH. Sequential deletion of C-terminus amino acids of the E1α component of the pyruvate dehydrogenase (PDH) complex leads to reduced steady-satte levels

of the functional E1$\alpha_2\beta_2$ tetramers: Implications for patients with PDH deficiency. Hum Mol Genet 2000;9:1041–1048. [PubMed: 10767328]

35. Han Z, Zhong L, Srivastava A, Stacpoole PW. Pyruvate dehydrogenase complex deficiency due to ubiquitination and proteosome-mediated degradation of the E1β subunit. J Biol Chem 2008;283:237–243. [PubMed: 17923481]
36. Methy D, Bertrand N, Prigent-Tessier A, Stanimirovic D, Beley A, Marie C. Differential MnSOD and HO-1 expression in cerebral endothelial cells in response to sublethal oxidative stress. Brain Res 2004;1003:151–158. [PubMed: 15019574]
37. Tabatabaie T, Potts JD, Floyd RA. Reactive Oxygen Species-Mediated Inactivation of Pyruvate Dehydrogenase. Arch Biochem Biophys 1996;336:290–296. [PubMed: 8954577]
38. Zaidan E, Sims NR. Reduced activity of the pyruvate dehydrogenase complex but not cytochrome c oxidase is associated with neuronal loss in the striatum following short-term forebrain ischemia. Brain Res 1997;772:23–28. [PubMed: 9406951]
39. Burger C, Gorbatyuk OS, Velardo MJ, Velardo MJ, Peden CS, Williams P, et al. Recombinant AAV viral vectors pseudotyped with viral capsids from serotypes 1, 2, and 5 display differential efficiency and cell tropism after delivery to different regions of the central nervous system. Mol Ther 2004;10:302–317. [PubMed: 15294177]
40. Grieger JC, Samulski RJ. Adeno-associated virus as a gene therapy vector: vector development, production and clinical applications. Adv Biochem Engin/Biotechnol 2005;99:119–145.
41. Gao G, Vandenberghe LH, Wilson JM. New recombinant serotypes of AAV vectors. Curr Gene Ther 2005;5:285–297. [PubMed: 15975006]

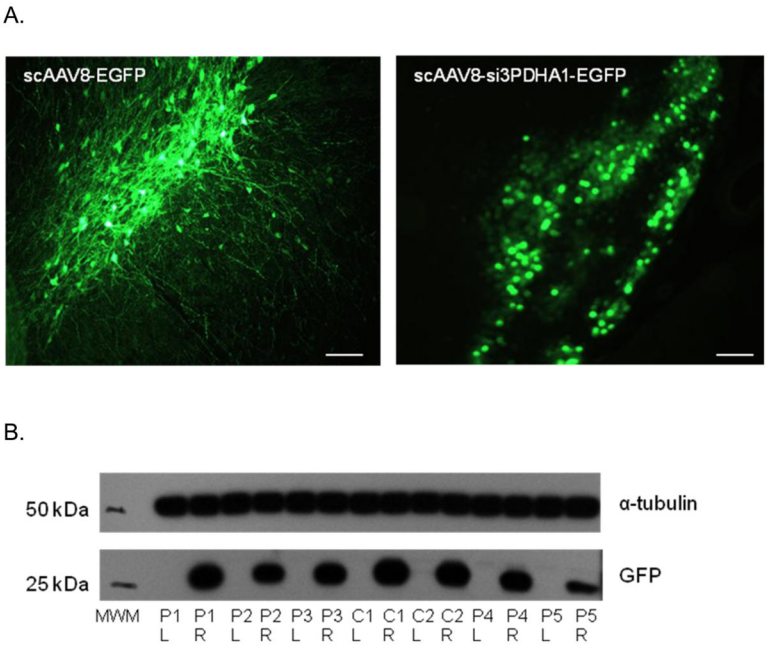

Fig. 1.

AAV8-mediated transgene expression in the SN and ST. (A) Representative direct fluorescent micrographs of SN section from AAV8-EGFP and AAV8-si3PDHA1-EGFP injected rats. Scale bar: 50 μm. (B) GFP protein expression in the ST detected by immunoblotting. P1 to P5 = AAV8-si3PDHA1-EGFP rat 1 to 5; C1 and C2 = AAV8-EGFP rat 1 and 2; L=left (uninjected); R=right (injected); MWM=molecular weight marker.

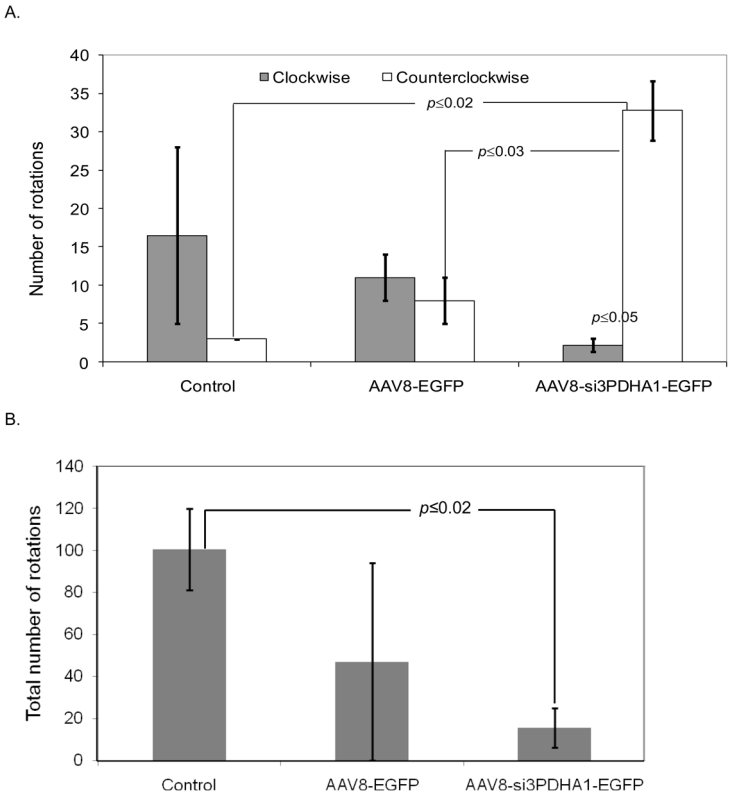

Fig. 2.

Amphetamine-induced rotational behavior 24 weeks after stereotaxic delivery of scAAV8-EGFP or scAAV8-si3PDHA1-EGFP in the rat's right ST and SN. **(A)** Number of clockwise and counterclockwise rotations 10 min after i.p. injection of amphetamine. **(B)** Total number of clockwise and counterclockwise rotations 20 to 90 min after amphetamine injection. Data are mean ± SEM of 2 rats for control and scAAV8-EGFP groups, and 5 rats for scAAV8-si3PDHA1-EGFP group. *P*-values indicate significant differences between the indicated treatment groups.

A.

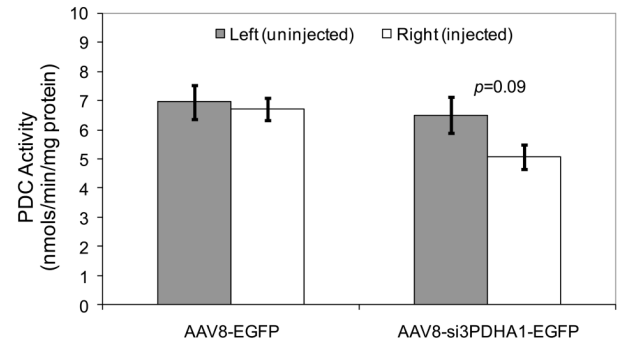

B.

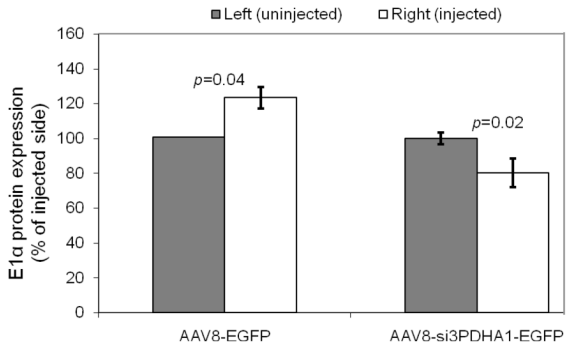

C.

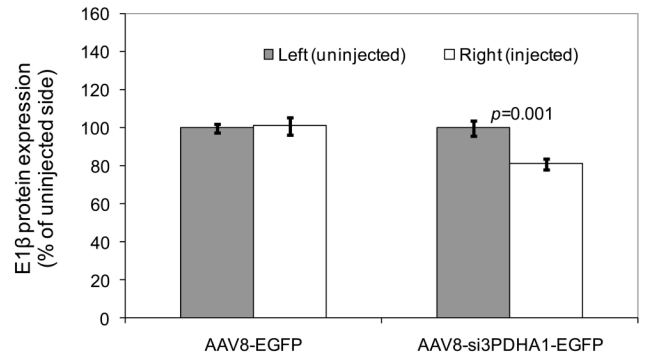

D.

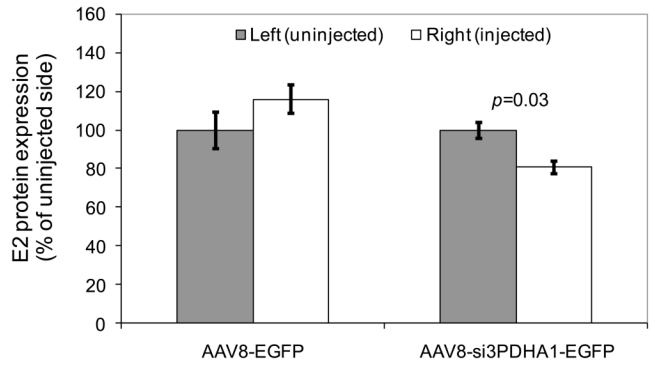

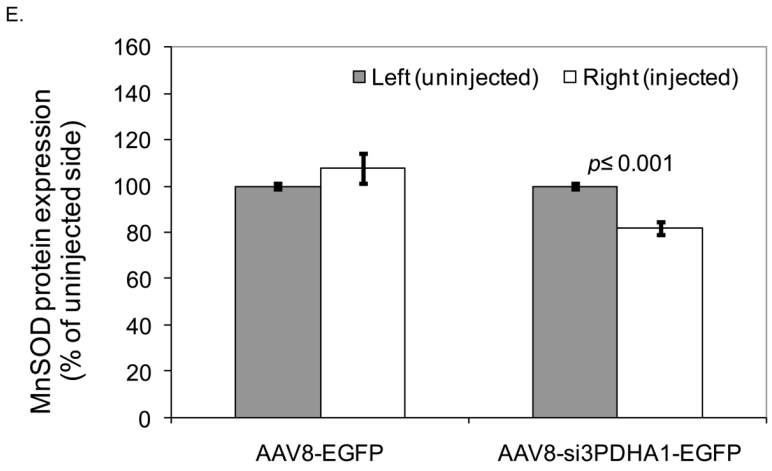

Fig. 3.

(A) Striatal PDC activity, and **(B–E)** expression of various proteins 14 weeks after rats were injected with scAAV8-EGFP (n=3) or scAAV8-si3PDHA1-EGFP (n=5) in the right ST and SN. Results are expressed as mean ± SEM. Striatal PDC activity was analyzed by measuring the rate of $^{14}CO_2$ formation from [1-^{14}C]-labeled pyruvate and samples were run in quadruplicate per sample, with appropriate blanks. For Western blots, quantitative analysis was carried out by measuring the pixel densities in each band (ImageJ) and the amount of protein was standardized to the amount of α-tubulin in each lane. Immunoblot data are means of two to three independent experiments. $p \leq 0.05$ denotes values that are statistically different between the indicated treatment groups.

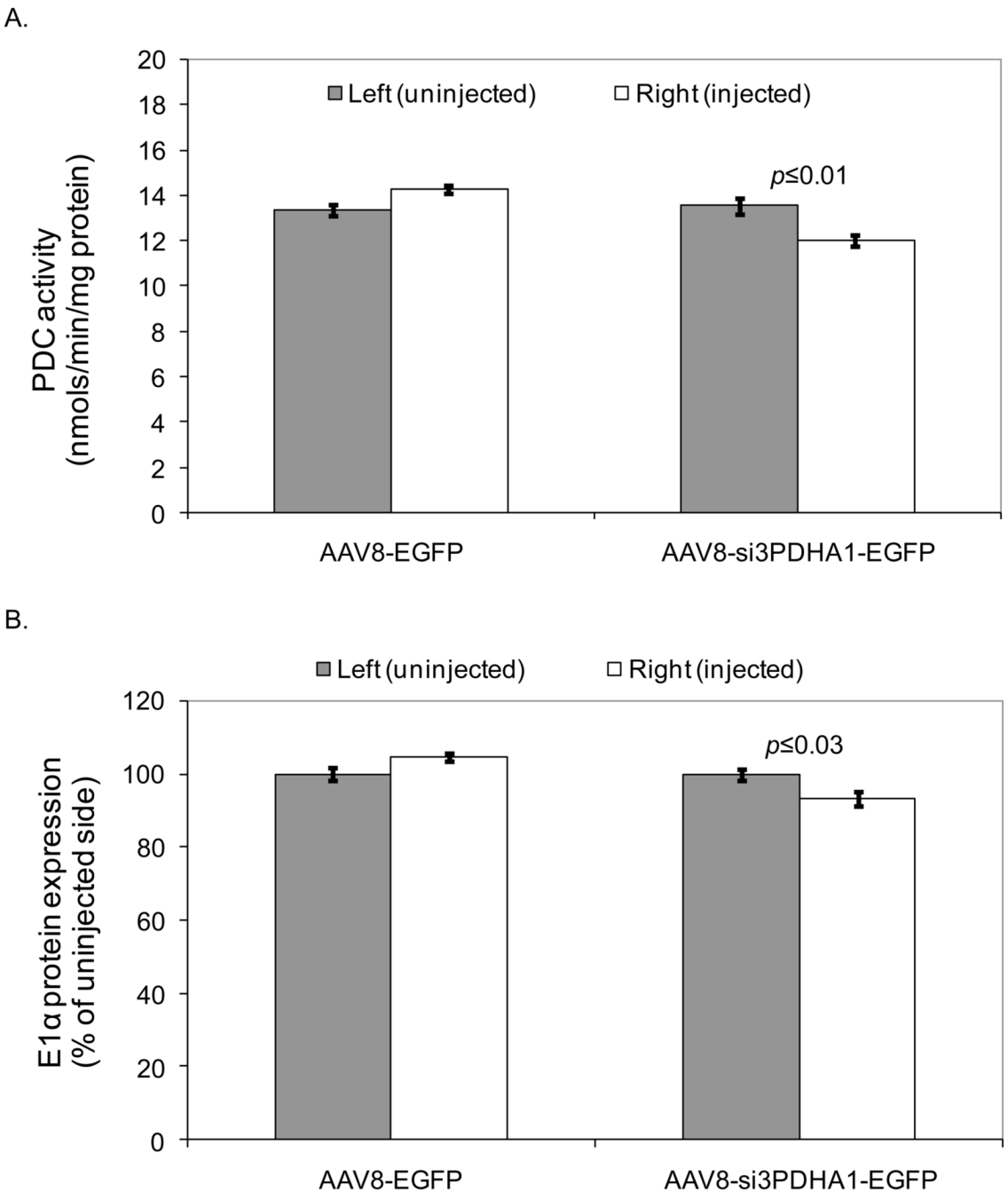

Fig. 4.

(A) Striatal PDC activity and **(B)** E1α protein expression 25 weeks after rats were injected with scAAV8-EGFP (n=2) or scAAV8-si3PDHA1-EGFP (n=5) in the right striatum and substantia nigra. Results are expressed as mean ± SEM. Striatal PDC activity was analyzed by measuring the rate of $^{14}CO_2$ formation from [1-^{14}C]-labeled pyruvate and samples were run in quadruplicate per sample, with appropriate blanks. For Western blots, quantitative analysis was carried out by measuring the pixel densities in each band (ImageJ) and the amount of protein was standardized to the amount of α-tubulin in each lane. Immunoblot data are means of two to three independent experiments. $p \leq 0.05$ denotes values that are statistically different between the indicated treatment groups.

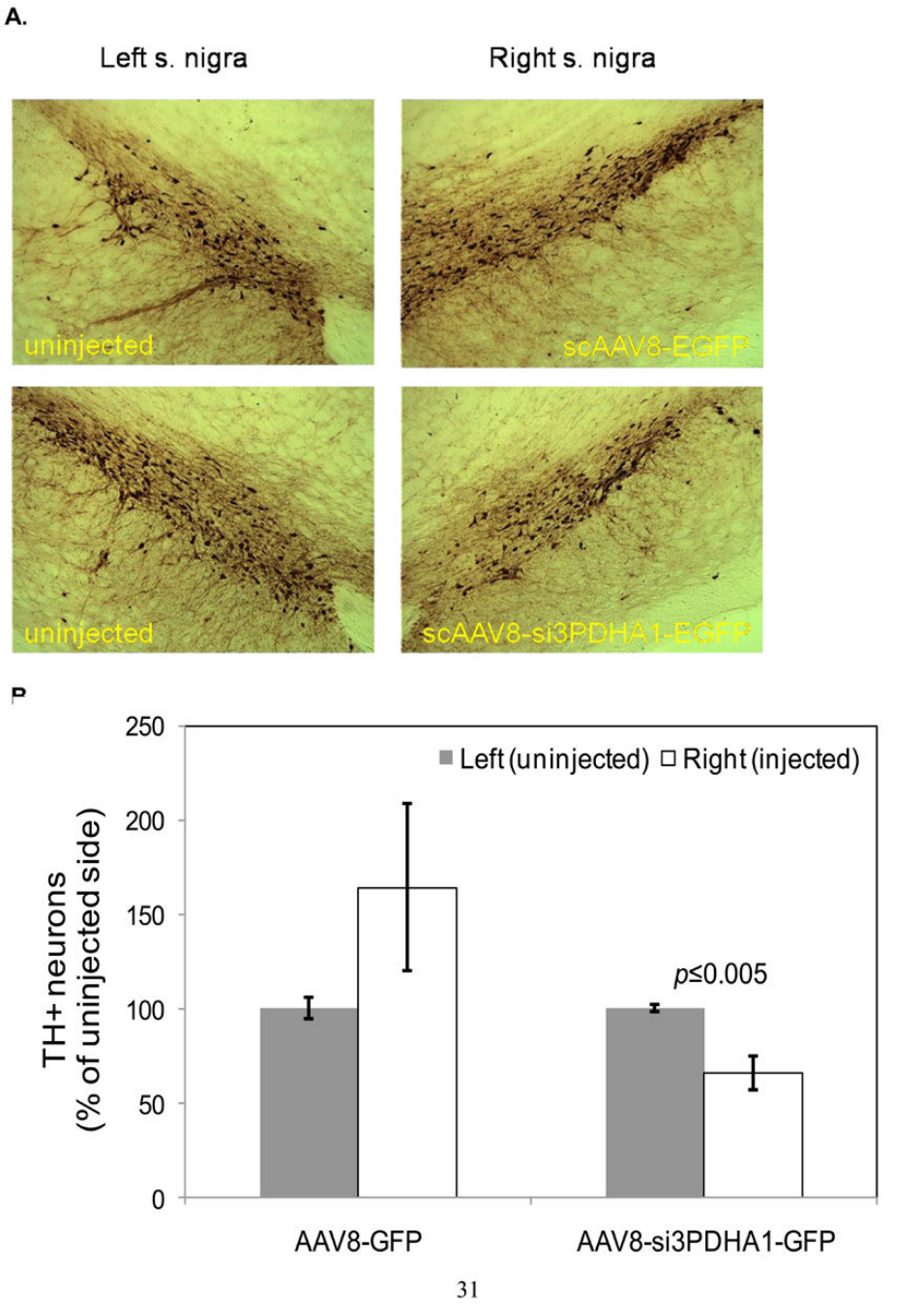

Fig. 5.

Nigral TH staining from a representative scAAV8-EGFP-injected control (**A**, upper column) and AAV8-si3PDHA1-EGFP- injected rat (**A,** lower column). **(B)** Unbiased estimation of nigral TH+ neuronal numbers in rats injected with scAAV8-EGFP (n=2) or scAAV8-si3PDHA1-EGFP (n=5). $p \leq 0.05$ denotes values that are statistically different between the indicated treatment groups.

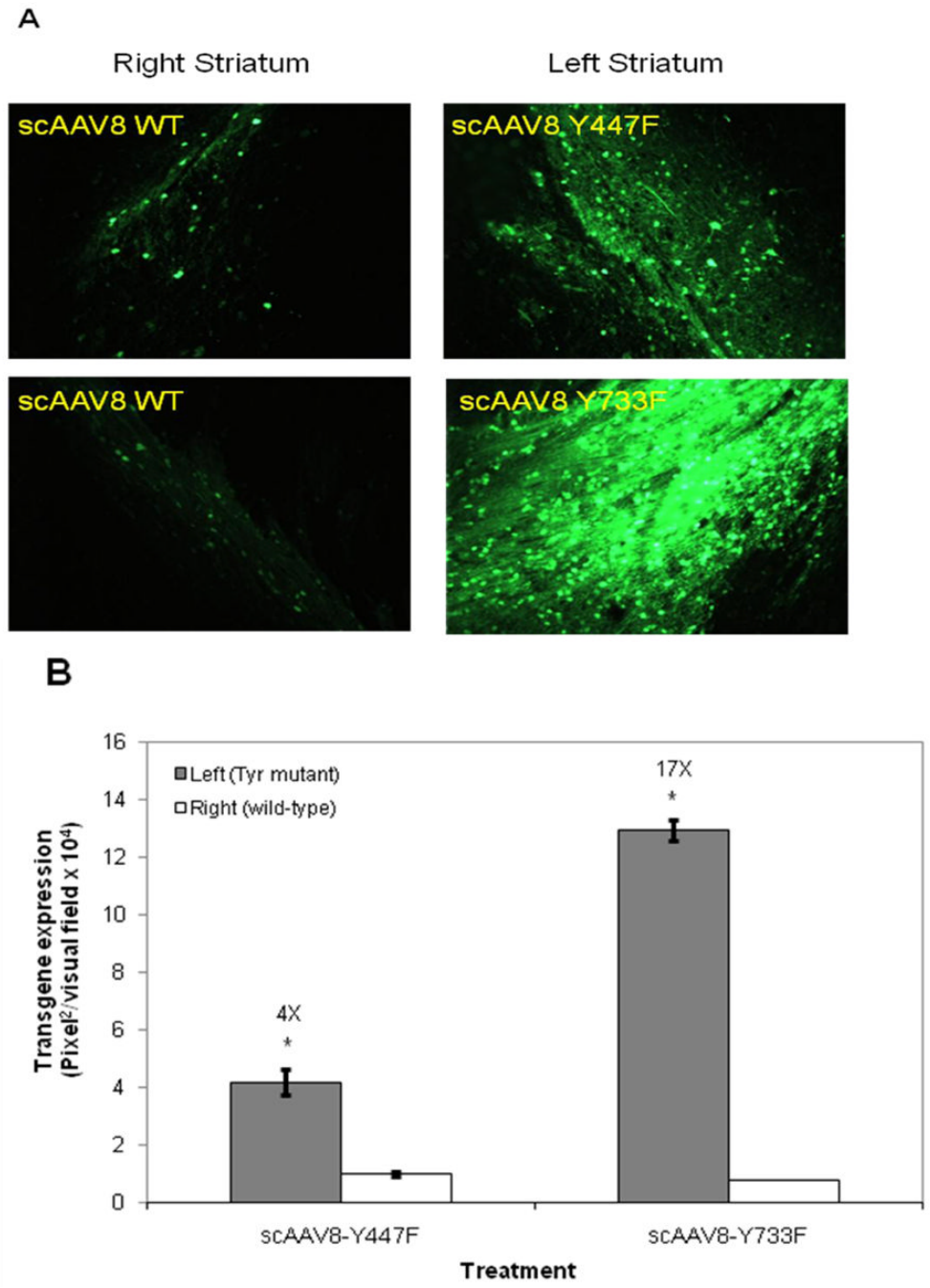

Fig. 6.

(A) scAAV8-mediated transgene expression in striatal neurons from rats injected with scAAV8-Y733F-EGFP tyrosine-mutant (left striatum) or wild-type (WT) scAAV8-EGFP (right striatum) vectors. Transgene expression was detected by fluorescence microscopy 6 weeks after injection of ~2×10^{10} viral particles per animal (n=3 per group; magnification, 20x). **(B)** Quantitative analyses of the transduction efficiency (ImageJ software). *$p \leq 0.002$ vs. WT scAAV8-EGFP.

Table 1

Nucleotide sequences of primers used for site-directed mutagenesis of surface-exposed tyrosine residues.

Mutants	Primer sequences (5'-3')
Y447F	
	Tyr→Phe *XbaI*
AAV8Y447-F	CCAGTACCTGTAC**TTC**TTGTCTAGAACTCAAACAACAGGAGG
AAV8Y447-R	CCTCCTGTTGTTTGAGTTCTAGACAAGAAGTACAGGTACTGG
Y733F	
	MluI Tyr→Phe
AAV8Y733-F	CCCCATTGGCACGCGTT**TC**CTCACCCGTAATC
AAV8Y733-R	GATTACGGGTGAGGAAACGCGTGCCAATGGGG

The codon triplets are shown in bold; red nucleotide denotes the mutation from phenylalanine to tyrosine (Y-F) residues. Green indicates the silent mutations to create the restriction enzyme sites shown (underlined), which were used to obtain the desired clone.